robotics

MDPI

Article

Kineto-Elasto-Static Design of Underactuated Chopstick-Type Gripper Mechanism for Meal-Assistance Robot

Tomohiro Oka [1,*], Jorge Solis [2], Ann-Louise Lindborg [3,4], Daisuke Matsuura [1], Yusuke Sugahara [1] and Yukio Takeda [1]

1 Department of Mechanical Engineering, Tokyo Institute of Technology, Tokyo 152-8552, Japan; matsuura.d.aa@m.titech.ac.jp (D.M.); sugahara.y.ab@m.titech.ac.jp (Y.S.); takeda.y.aa@m.titech.ac.jp (Y.T.)
2 Department of Engineering and Physics, Karlstad University, 651 88 Karlstad, Sweden; jorge.solis@kau.se
3 Camanio Care AB, 131 30 Nacka, Sweden; annlouise.lindborg@camanio.com or ann-louise.lindborg@mdh.se
4 School of Innovation, Design and Engineering, Mälardalen University, 721 23 Västerås, Sweden
* Correspondence: tomohiro.oka.822@gmail.com; Tel.: +81-3-5734-2177

Received: 28 May 2020; Accepted: 28 June 2020; Published: 30 June 2020

Abstract: Our research aims at developing a meal-assistance robot with vision system and multi-gripper that enables frail elderly to live more independently. This paper presents a development of a chopstick-type gripper for a meal-assistance robot, which is capable of adapting its shape and contact force with the target food according to the size and the stiffness. By solely using position control of the driving motor, the above feature is enabled without relying on force sensors. The gripper was designed based on the concept of planar 2-DOF under-actuated mechanism composed of a pair of four-bar chains having a torsion spring at one of the passive joints. To clarify the gripping motion and relationship among the contact force, food's size and stiffness, and gripping position, kineto-elasto-static analysis of the mechanism was carried out. It was found from the result of the analysis that the mechanism was able to change its gripping force according to the contact position with the target object, and this mechanical characteristic was utilized in its grasp planning in which the position for the gripping the object was determined to realize a simple control system, and sensitivity of the contact force due to the error of the stiffness value was revealed. Using a three-dimensional (3D) printed prototype, an experiment to measure the gripping force by changing the contact position was conducted to validate the mechanism feature that can change its gripping force according to the size and the stiffness and the contact force from the analysis results. Finally, the gripper prototype was implemented to a 6-DOF robotic arm and an experiment to grasp real food was carried out to demonstrate the feasibility of the proposed grasp planning.

Keywords: mechanism design; meal-assistance robot; chopstick-type gripper; under-actuated mechanism; kineto-elasto-static analysis; grasp planning

1. Introduction

WHO (World Health Organization), or rather the WHOQOL (World Health Organization Quality of Life) group, has developed a test instrument to evaluate the quality of life, as a complement to a standard health assessment. The instrument had questions within the following domains: physical, psychological, level of independence, social relationships, environment, and spirituality/religion/personal beliefs. Within the domain "level of independence" WHO has the following facets: mobility, activities

of daily living, dependence on medicinal substances and medical aids, dependence on non-medical substances (alcohol, tobacco, drugs), communication capacity, and work capability [1]. The independency and possibility to manage activities of daily living are taken into account as one of the important abilities.

Undernutrition is a serious problem amongst the elderly. For example, elderly people in Scandinavia have a high risk of malnutrition and eating difficulty is a risk factor for it according to Nyberg et al. [2]. Japan and Sweden share the same problem with the demographical development, and both countries are robot and technical-friendly. This gives a common goal to manage to take care of the elderly.

Up to now, several robotic systems for eating have been introduced. Handy 1 is an assisting robotic system, which is composed of a robotic arm that works with different trays, depending on the task. For eating, it has a tray with different compartments, where different kinds of food can be placed and the user chooses what compartment to take from. It was also designed to assist other activities than eating, such as drinking, and make-up application, which requires different kinds of detachable slide-on tray sections and end effectors [3]. Developments of robotic assistive eating devices with chopstick-type gripper have been done in Japan [4]. The mechanism in [4] is based on an industrial robot-like arm. The meal assistance robot "My Spoon" is composed of a manipulator arm with 5-DOFs and an end-effector that is controlled by a joystick. As the end effector has a spoon and a fork that together work as a pincer, it picks up food between the spoon and fork and lifts it up to the mouth and, when the user touches the spoon, the fork folds back to release the bite. The food is put into a box with four compartments [5,6]. The "Neater Eater" started as a 2-DOF arm robot with a spoon as the end-effector, which is moved by the user with a damping mechanism that absorbs tremor [7]. Now that the Neater Eater robotic V6 has been developed [8]. It takes the food by turning the plate and scrape towards the brim and can be controlled by a touch screen. The "Meal Buddy" has a 3-DOF robotic arm and a spoon as the end-effector, and it has three bowls for the food that are mounted on a board using magnets. It is possible to choose different ways of control devices [9]. "Obi" is one of the newest eating devices on the market. Obi's base shape has similarities to a drop and the arm is situated on the right side of the plate that has four compartments/bowls to put the food in. It is white and has 6-DOF. It is controlled by the user with two buttons, one for choosing which one of the four compartments with food to take from, and the other button for starting the grasping of food and lifting to the mouth. The LARM [10] clutched arm is driven by a single actuator from which the motion is transmitted to its joints with the help of gears and electromagnetic clutches. The arm has a parallelogram-based mechanism for the limb part, which drives the upper arm and forearm from the shoulder. Even though the kinematic design has been considerably simplified, the system can be only used for eating and the end-effector cannot adapt to the stiffness of the grasped food. An assistive robot for self-feeding that is capable of handling Korean food, including sticky rice, has been introduced in [11]. It is composed of a dual-arm manipulator with a total of 6-DOF (without the gripper). The first robotic arm (spoon-arm) uses a spoon to transfer the food from a container on a table to the user's mouth. The second robotic arm picks food up from a container and then puts it on the spoon of a spoon-arm. The level of cognitive load to the user increases and two different tools are required while eating due to the use of the dual-arm manipulation.

In most cases mentioned above, meal assistant robots/systems are basically composed of a robot arm to move the gripping tool of foods, such as spoon and chopsticks. From the point of view of real use of meal assistant robot for the promotion of independent life of elderly, it is very important to consider safety, how it looks, sounds, and so on, as well as the complexity of the mechanical design, the total cost of the system and power consumption.

Based on the background and discussions mentioned above, we have undertaken development/research in order to promote an independent life of elderly people by a multi grip tool to facilitate eating. To raise the standard of living of the elderly from the viewpoint of eating habits, Japan–Swedish industry-academia collaboration program began in 2017 [12]. In this project, we used the eating aid Bestic. The initiative

to Bestic came from Sten Hemmingsson, who had the need for the product himself and who wanted to be able to continue eating independently. The product development is described in the report "Bestic An eating-aid for persons with little or no ability to move their arms" [13]. The product has continued developing with the influence of users [14]. Our research team aimed to expand its function by attaching a gripper instead of a spoon to Bestic developed at Camanio Care AB in Sweden.

We aimed to enhance the functionalities of Bestic in order to enable frail elderly to have an independent meal experience and reduce caregiver's burden. For this purpose, in this research, we aimed to further develop the current commercial version of Bestic for targeting current Bestics' users as well as frail and dependent elderly. Therefore, we focused on developing different kinds de-attachable multigrip tools that can passively adapt to the stiffness of the grasped object as well as integrating the vision system for enhancing the usability of the proposed system (e.g., vision-based control). In particular, in this research, we aimed to adapt the eating device Bestic to Japanese eating customs, and we developed a chopstick-type gripper that allows users to properly eat Japanese food as well as to perform other daily life activities.

Regarding multigrip tools, chopsticks are widely used because of its usefulness in picking up many kinds of foods and its very simple composition. Although using chopsticks looks like needing dexterous operation by human's fingers, since it can be used to do various manipulation of foods, such as picking up, cutting, sticking, and so on; it can actually be used easily once the purpose of use has been adequately narrowed. In this paper, we rather focus on the picking up operation of chopsticks and propose a reasonable design of a gripper mechanism that employs an under actuation principle to make the gripper adaptable against various size and stiffness of foods by solely using position control and without introducing force sensors. "Solely use" means that the gripper only has "open" or "close" states, and a control system only gives maximum or minimum positions to the actuator corresponding to each state. In order to calculate the configuration of the mechanism against the given property of the target food and the actuator input, and to figure out a suitable design of the gripper and grasp planning which derives the motor input angle and the contact position with the target object, in order to realize a simple control system, Kineto-elasto-static analysis was performed in this paper. Also, an effect of the stiffness error on the gripping force is investigated. An experiment using the prototype to measure the contact force was conducted to validate the modeling of the mechanism and the feature of the mechanism obtained by the kineto-elasto-static analysis. Finally, the gripper prototype was implemented in a 6-DOF robotic arm and the grasp planning experiment was carried out to demonstrate the feasibility of the proposed grasp planning.

2. Meal-Assistance Robot and Multi-Gripper

2.1. Composition of the Meal-Assistance Robot with Vision System and Multi-Gripper

The proposed system is composed of Bestic arm, a mini PC (NUC6i5SYK), a camera (Intel Real Sense SR300), an articulated arm with camera attachment (with passive joints), and different kinds of de-attachable multrigrip tools, different kinds of de-attachable multrigrip tools (e.g., spoon, chopstick-type, etc.), as shown in Figure 1. A vision-based feature extraction algorithm for estimating the location of the food on the plate has been developed by extracting the color feature [15]. After detecting the location of the object to be grasped, by means of a proposed distributed vision-based control system, the coordinates (x and y) are then transmitted to the control system of Bestic [15].

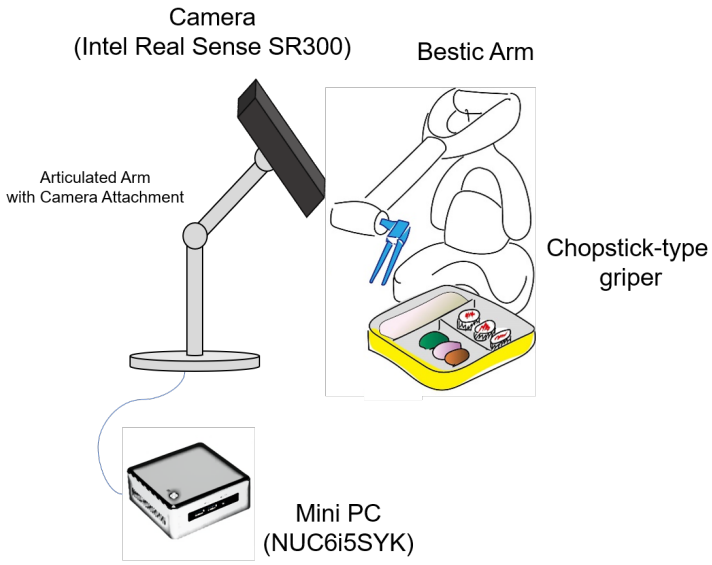

Figure 1. Proposed robot system.

2.2. Requirement to the Multi-Gripper

In our research, we consider the following major constraints to the multigrip tools in order to adapt the new functionalities to the present Bestic:

1. It shall only be powered by the motor that normally drives the spoon.
2. It shall be possible to grasp Japanese foods that are hard to manipulate with a spoon.
3. It shall be easy to clean.
4. It shall both be possible to pick up food on a plate and then release it in the mouth of a user.
5. It shall be possible to be taken off for replacement to different tools like a toothbrush for example.

In the following part of the paper, we will focus on the design and grasp planning of the chopstick-type gripper while taking into account these constraints explained above.

2.3. Design Requirements to the Chopstick-Type Gripper

The gripper for the meal-assistance robot is required to adjust its gripping force according to foods. Each food has its size, mass, and stiffness, which is a problem for the gripper to adjust the gripping force. Using a force sensor for controlling the gripping force leads to high cost and complexity of the system, which makes the robot unaffordable for users. In addition, it seems hard to prepare a precise database of physical property of foods for the control of the gripping force, because the number of food types is enormous, even if only Japanese food is considered. Thus, a chopstick-type gripper that enables adjusting the gripping force according to food's size and stiffness without any force sensors is required. In this paper, a mechanism that is based on the concept of under-actuation is proposed and analyzed to achieve passively adjust its gripping force while using an elastic element, and grasp planning is investigated.

3. Chopstick-Type Gripper Mechanism

Figure 2 shows the proposed mechanism. It is a planar 2-DOF mechanism composed of two four-bar closed loops, ABCD (Loop 1) and BEFC (Loop 2). The degree of freedom of this mechanism is calculated while using Gruebler's equation described as Equation (1).

$$F = 3(N - J - 1) + \sum_{i=1}^{J} f_i = 3(7 - 8 - 1) + 8 = 2 \quad (1)$$

where, N is the number of links, and J is the number of joints, and $f_i (i = 1 \sim J)$ is the degree of the freedom of the joint. In this case, all of joints are revolute pairs, thus $f_i = 1 (i = 1 \sim J)$.

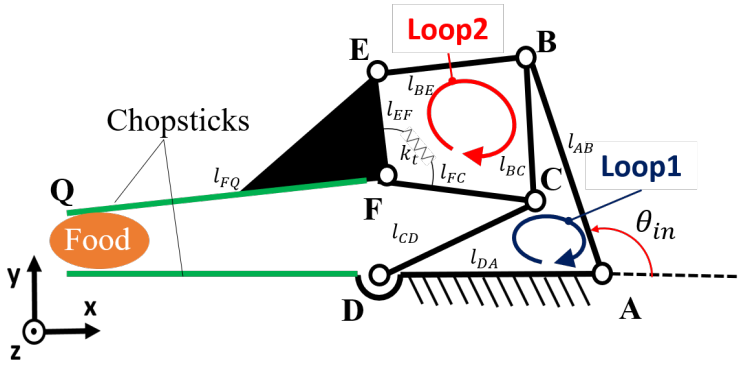

Figure 2. Proposed mechanism of the gripper.

A pair of chopsticks is comprised of the base link AD with an extension and the coupler link FQ. All joints A to F are revolute-type, and only one of them, A, is actuated. Thus, te entire mechanism is under-actuated [16–19], but, since a torsion spring is attached at joint F, connecting the links FC and FE, its configuration is statically determined once the actuator's input angle and external force on the end-effector (gripping force between chopsticks) are specified. When the chopsticks are not in contact with the food and no external force is applied, joint F is considered to remain at a neutral angle determined by the torsion spring, and the mechanism's configuration is thus only determined by the input angle of the actuator. In contrast, when the chopsticks contact with the food, the shape of Loop 2 changes according to the deformation of the torsion spring due to a deterministic motion of Loop 1. Thus, Loop 1 generates the path of the tip of the chopsticks part, and Loop 2 regulates the gripping force with an object to be grasped. Therefore, the gripping force is adjustable by the position control of the driving motor, and each of the loops can be separately designed. Additionally, the proposed mechanism has a feature to grasp an object at the tip part and adjust its force with deformation of the torsion spring, while the other underactuated mechanisms, such as [16–19], were designed to wrap around an object to grasp it.

4. Kineto-Elasto-Static Analysis of the Mechanism

This section addresses the kineto-elasto-static analysis of the proposed gripper mechanism. For the analysis, the model includes the contact point with the object to be grasped, and the object is modeled as a simple compression spring. The solution of the analysis is obtained from the condition that satisfies both the geometrical and mechanical relationship of the system. A simple computational scheme is needed in order to reduce the calculation time. In our previous paper [20], we presented an analysis scheme where L and ϕ are estimated from an assumed w and the assumed w is iteratively adjusted until the contact force is converged. However, it suffered a high computational cost. In the present paper, a new analysis scheme that needs less calculation cost is introduced, and the calculation performance is compared with

our previous analysis scheme. Using the analysis, the relationship among the contact force of the gripper, the size and the stiffness of food, and the contact position is obtained to propose a grasp planning scheme.

4.1. Modeling of the Mechanism Including the Contact point

Under the assumption that food to be picked up is an elastic body, a kineto-elasto-static model, including the chopstick mechanism and food, is set as shown in Figure 3. In order to take the relative motion between the food and the chopsticks into account, a prismatic pair and a revolute pair are set at the contact point between the food and the end-effector of the mechanism on the link FQ, and the joint is set as P. A distance between joint F and joint P, and an angle of FP against the horizontal (x) axis are denoted as L and ϕ, respectively, and these parameters are set as unknown. f stands for the contact force. Its direction is considered to be normal to FQ, and the magnitude is denoted by a scalar f [N]. A target food is modeled as a vertical spring of which the length is set as w and the spring constant is set as K [N/m], and with its one end point fixed on the base link AD at $(x_P, 0)$. Subsequently, the position of P is set as (x_P, w), using h, which is set as the distance from the tip and the P in x-axis direction. The initial size and deformation of the food are denoted as w_o [mm] and Δw [mm], respectively. The angle θ_B between links BE and BC and the virtual external torque M_{EX}, which is added for the sake of convenience and its value should be zero, are introduced. In this paper, assumptions are made that the mechanism moves quasi-statically in the horizontal plane where the inertial and gravitational forces and viscosity of the food can be neglected. Additionally, as for the balance of forces between the contact force and the reaction force from the food, only the y-axis component is considered, and the x-axis component is ignored, since the one end of the spring is considered being fixed on the base link AD.

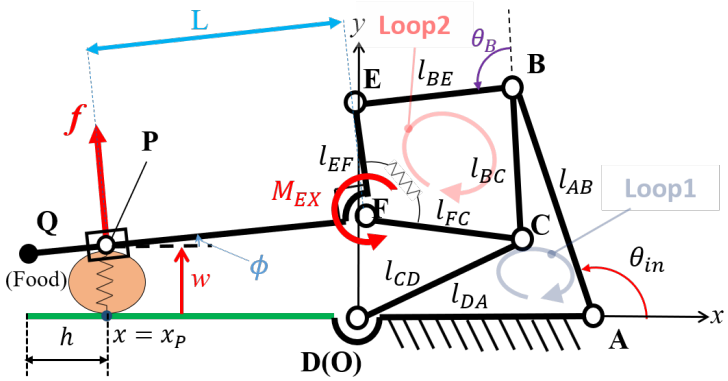

Figure 3. Modeling of the mechanism including the contact point.

4.2. Analysis Scheme Introducing a Virtual Torque

The analysis scheme is referenced to [21,22] in that an additional parameter of force is set to satisfy the mechanical condition. When the input motor angle θ_{in} is given, using one parameter, all of the position of the joints can be determined, since the whole system has 2-DOF. In the analysis scheme, the angle θ_B is set as the convergence parameter for determining the joint positions of the system.

Once the x-position (x_P), initial size w_o, and the stiffness K of the target food are given, the configuration of the mechanism and contact force for a given input angle θ_{in} can be obtained according to the procedure described below and are shown in Figure 4.

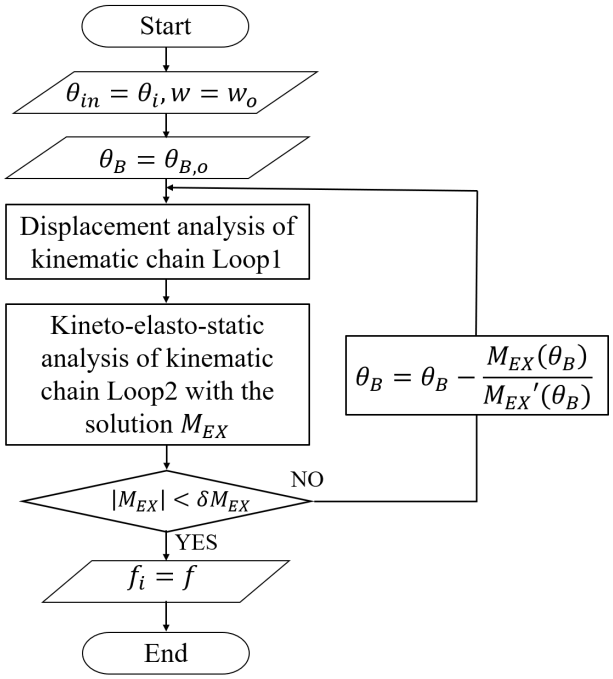

Figure 4. Flow chart of the analysis scheme.

1. With the input angle θ_{in}, the displacement of the kinematic Loop 1 is determined. Note that θ_i is the input angle of which value is between the given initial position to the given final position.
2. The x-position of the target x_P is given, same as the x-position of point P.
3. The statistic force analysis of the kinematic Loop 2 is carried out with joint positions described with the parameter θ_B. When considering the equilibrium of force and moment on each link, simultaneous equations that include the virtual external torque M_{EX} on joint F and the x-component and y-component forces at the joints B, C, E, and F as unknown are formulated. Subsequently, the value of M_{EX} can be calculated.
4. When the absolute value of M_{EX} is smaller than the threshold δM_{EX}, the calculation is terminated, and the value f can be described with the parameter θ_B at that time. When its value exceeds δM_{EX}, adjustment of the value of θ_B is done and the calculation is repeated back to step 3 until the process converges.

Let us think of Loop 2, which is a four-bar mechanism with 1-DOF. When the parameter θ_B is given, positions of joints E and F can be determined as functions of θ_B, $\boldsymbol{E} = \boldsymbol{E}(\theta_B)$,$\boldsymbol{F} = \boldsymbol{F}(\theta_B)$. By using them, position of joint P can be described as Equation (2) under consideration of the geometric relations of Loop 2,

$$\boldsymbol{P} = \boldsymbol{F}(\theta_B) + \frac{L}{l_{EF}} R(\angle EFQ) \cdot (\boldsymbol{E}(\theta_B) - \boldsymbol{F}(\theta_B)) = \begin{bmatrix} P_x \\ P_y \end{bmatrix} = \begin{bmatrix} x_p \\ w \end{bmatrix} \tag{2}$$

where, $R(\angle EFQ)$ represents a rotational matrix in respect to $\angle EFQ$.

Because P_x is the same as the given x_P, L can be obtained from Equation (2) when considering the x components. L can therefore be considered to have another function with respect to θ_B, $L(\theta_B)$. Accordingly, the size of food w and position of P can also be obtained as the function of θ_B, $w = w(\theta_B)$ and $\boldsymbol{P} = \boldsymbol{P}(\theta_B)$, considering the y components of Equation (2). Additionally, the angle θ_{EFC} between links EF and FC and the angle ϕ are expressed as $\theta_{EFC} = \theta_{EFC}(\theta_B)$, $\phi = \phi(\theta_B)$. In this analysis scheme, it is set that the contact

force from the gripper and the reaction force from the food are balanced in the y-direction, then their relationship is described as;

$$f\cos\phi = K(w_o - w). \tag{3}$$

From these geometrical and mechanical relations, the magnitude f and the torque τ_k of the torsion spring are obtained as;

$$\begin{aligned} f(\theta_B) &= \frac{K(w_o - w(\theta_B))}{\cos\phi(\theta_B)}, \\ \tau_k(\theta_B) &= k_t(\theta_{EFC,initial} - \theta_{EFC}(\theta_B)). \end{aligned} \tag{4}$$

From the free body diagram of Loop 2 that is shown in Figure 5, the equilibrium of the force and moment on each link is formulated, as follows.

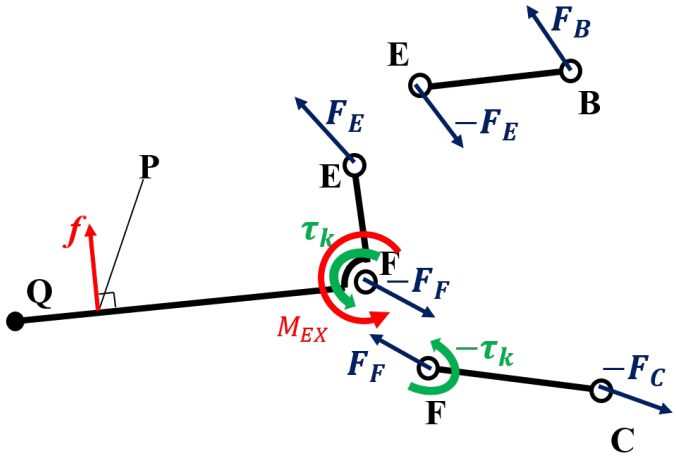

Figure 5. Free body diagram included virtual torque M_{EX}.

Link BE:

$$\left.\begin{aligned} \boldsymbol{F_B} - \boldsymbol{F_E} &= \boldsymbol{0} \\ (\boldsymbol{E}(\theta_B) - \boldsymbol{B}(\theta_B)) \times (-\boldsymbol{F_E}) &= 0 \end{aligned}\right\} \tag{5}$$

Link EFQ:

$$\left.\begin{aligned} \boldsymbol{F_E} - \boldsymbol{F_F} + f(\theta_B)\boldsymbol{e}(\theta_B) &= \boldsymbol{0} \\ \tau_k(\theta_B) + (\boldsymbol{E}(\theta_B) - \boldsymbol{F}(\theta_B)) \times \boldsymbol{F_E} - f(\theta_B)L(\theta_B) + M_{EX} &= 0 \end{aligned}\right\} \tag{6}$$

Link FC:

$$\left.\begin{aligned} \boldsymbol{F_F} - \boldsymbol{F_C} &= \boldsymbol{0} \\ -\tau_k + (\boldsymbol{C}(\theta_B) - \boldsymbol{F}(\theta_B)) \times (-\boldsymbol{F_C}) &= 0 \end{aligned}\right\} \tag{7}$$

From Equations (4) to (7), simultaneous equations are obtained as the following Equation (8).

$$A(\theta_B)\begin{bmatrix} \boldsymbol{F_B} \\ \boldsymbol{F_E} \\ \boldsymbol{F_F} \\ \boldsymbol{F_C} \\ M_{EX} \end{bmatrix} = \boldsymbol{b}(\theta_B) \tag{8}$$

where,

$$A(\theta_B) = \begin{bmatrix} 1 & 0 & -1 & 0 & 0 & 0 & 0 & 0 & 0 \\ 0 & 1 & 0 & -1 & 0 & 0 & 0 & 0 & 0 \\ 0 & 0 & y_E(\theta_B) - y_B & -(x_E(\theta_B) - x_B(\theta_B)) & 0 & 0 & 0 & 0 & 0 \\ 0 & 0 & 1 & 0 & -1 & 0 & 0 & 0 & 0 \\ 0 & 0 & 0 & 1 & 0 & -1 & 0 & 0 & 0 \\ 0 & 0 & -(w(\theta_B) - y_F(\theta_B)) & x_P(\theta_B) - x_F(\theta_B) & 0 & 0 & 0 & 0 & 1 \\ 0 & 0 & 0 & 0 & 1 & 0 & -1 & 0 & 0 \\ 0 & 0 & 0 & 0 & 0 & 1 & 0 & -1 & 0 \\ 0 & 0 & 0 & 0 & 0 & 0 & y_C - y_F(\theta_B) & -(x_C - x_F(\theta_B)) & 0 \end{bmatrix}$$

$$\boldsymbol{b}(\theta_B) = \begin{bmatrix} 0 & 0 & 0 & 0 & 0 & -\tau_k(\theta_B) + f(\theta_B)L(\theta_B) & 0 & 0 & \tau_k(\theta_B) \end{bmatrix}^T$$

By solving Equation (8), $M_{EX} = M_{EX}(\theta_B)$ is obtained. When the reaction force from the target food and torque of the torsional spring are balanced, value of M_{EX} should be zero. A numerical computation based on Newton-Raphson method [21] can solve this equation regarding $M_{EX}(\theta_B) = 0$.

4.3. Comparison of the Computational Efficiency

In Figure 6, the computational efficiency of the analysis scheme is compared with the scheme of [20]. Design parameter values, such as link lengths, are given in Table 1. By using the simulation based on the kinematic analysis, the initial position of the motor as 109 deg and the final position as 117.5 deg were decided. As the motor angle is 117.5 deg, the gripper is closed and the tip of the chopstick part (point Q) reaches the other tip of the chopstick part of link AD, when there is no target object between the chopstick parts. These parameters are obtained through the process that is explained in the following section.

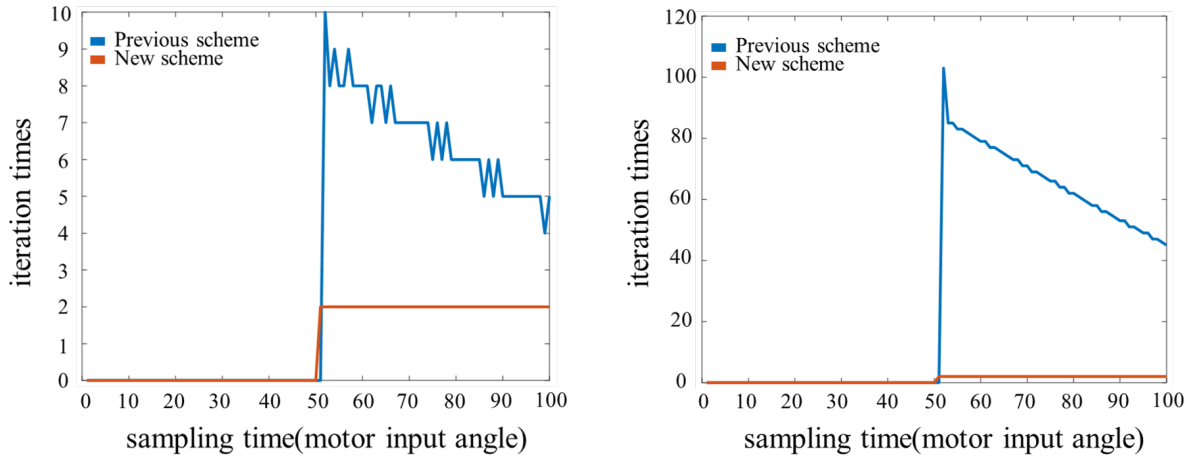

(**a**) Scale of threshold value is 1.0×10^{-3}.

(**b**) Scale of threshold value is 1.0×10^{-4}.

Figure 6. Comparison of iteration times among the analysis schemes.

Table 1. Parameters of the mechanism.

Parameter	Value	Parameter	Value
l_{AB}	31 mm	l_{BE}	24 mm
l_{BC}	24 mm	l_{EF}	12 mm
l_{CD}	24 mm	l_{FC}	22 mm
l_{DA}	34.5 mm	l_{FQ}	115.5 mm
$k_t = 3.52 \times 10^{-2}$ Nm/rad		$\angle \mathrm{EFC} = \pi/2$ rad	

Figure 6 shows the iteration times against the sampling time (which corresponds to the input motor angle). The sampling time is set as 0 when the motor input angle is initial position (109 deg) and as 100 when the motor input angle reaches the final position (117.5 deg), and intermediate values are linearly ramped. The parameters used in the analysis methods are set as $w_o = 15$ mm, $K = 1.0 \times 10^3$ N/m, $h = 5$ mm. Note that δf is the threshold vale for the convergence judgement used in [20]. In order to match the scales of threshold value used in the two analysis schemes, in Figure 6a $\delta f = 1.0 \times 10^{-3}$N, $\delta M_{EX} = 1.0 \times 10^{-3}$ Nm are used, and in Figure 6b $\delta f = 1.0 \times 10^{-4}$ N, $\delta M_{EX} = 1.0 \times 10^{-4}$ Nm are used for the computations. Figure 6a shows that the iteration times in the new scheme are constant as 2, while the iteration times in the previous scheme are decreasing from 10 as the sampling time increases, and the new scheme's computational times are less than the previous scheme's ones. Figure 6b shows that the iteration times in the new scheme are constant as 2, likewise Figure 6a, while the iteration times in the previous scheme are decreasing from 100 as the sampling time increases, and the new scheme's computational times are less than the previous scheme's ones. These results are caused by that in the previous scheme the parameter w is changed by the fixed value, while in the new scheme the parameter θ_B is changed by Newton-Raphson method. Also, in the previous scheme, it is needed to solve the complex non-linear simultaneous equation, while, in new scheme, it is needed to solve the simple equation as Equation (8), and then it can be said that the cost of calculation of the new scheme is less than the one of the previous scheme. Therefore, the new analysis scheme is better than the previous scheme with respect to the computational efficiency. The new analysis scheme is used in the following part of this paper.

4.4. Numerical Example

Numerical examples are shown, in which the analysis scheme that is described in the previous section is applied. The results are obtained by a numerical software MATLAB. Design parameter values, such as link lengths, are given in Table 1, and δM_{EX} and $\delta\theta_B$ are set as $\delta M_{EX} = 1.0 \times 10^{-10}$ Nm, $\delta\theta_B = 1.0 \times 10^{-10}$ rad, respectively.

Figure 7 shows a result of the magnitude of contact force f against the initial food size w_o and the food stiffness K when the input angle reaches the preliminarily determined target value ($\theta_{in} = 117.5$ deg). In this analysis, ranges of w_o and K are set as 1 mm to 20 mm and 0.01×10^3 N/m to 1.0×10^3 N/m, respectively. The numerical calculation was carried out with 100 divisions on each parameter. From the result, it is figured out that the bigger initial size and stiffness result in the larger magnitude of the contact force. The contact force seems to be constant for a wide range of stiffness among the range of w_o between 2 mm and 4 mm. In the range of w_o between 4 mm and 11 mm, the contact force increases according to the increments of the stiffness. Among the range of w_o between 11 mm and 20 mm, while the contact force increases sharply within the range of K up to around 0.3×10^3 N/m, it increases smoothly in the other range of K. Additionally, the magnitude of force f increases monotonically as the value of the initial food size w_o increases.

Figure 8 shows the relation between contact force f [N], food's stiffness K [N/m] and the contact point h [mm]. At this time, the input angle of the driving motor θ_{in} is set as 117.5 deg, and the initial size of food w_o is varied as 5 mm, 10 mm, 15 mm, 20 mm. From these results, it is figured out that the magnitude

of force f increases monotonically as the value of the distance from the tip h [mm] increases. In other words, it can be said that the larger distance between the contact point and the tip of the chopstick part, the larger force the mechanism outputs. Additionally, it can be said that the gripper mechanism is able to change its gripping force actively by changing the position of the contact point, and this mechanism's feature can be utilized for a grasping planning in the following section.

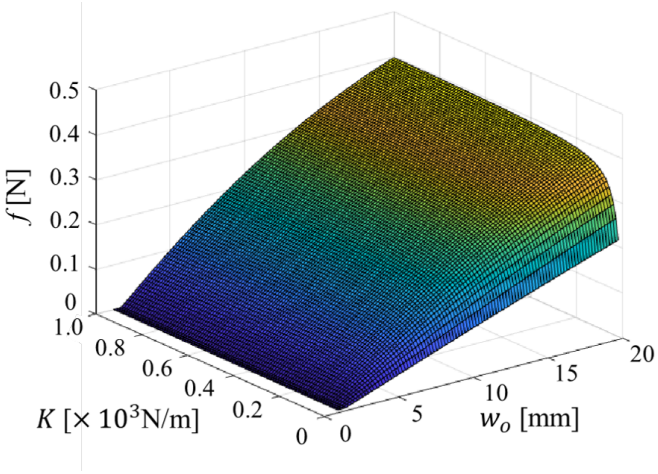

Figure 7. Relation between contact force f and food's size w_o, food's stiffness K as $\theta_{in} = 117.5$ deg.

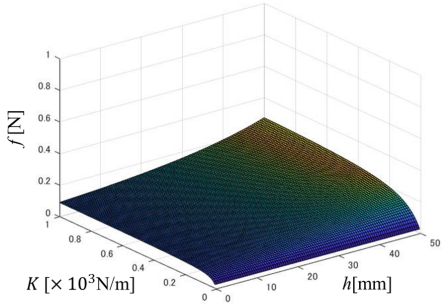

(**a**) $w_o = 5$ mm

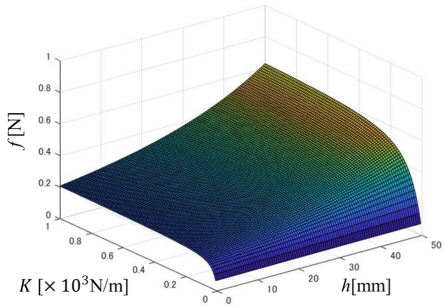

(**b**) $w_o = 10$ mm

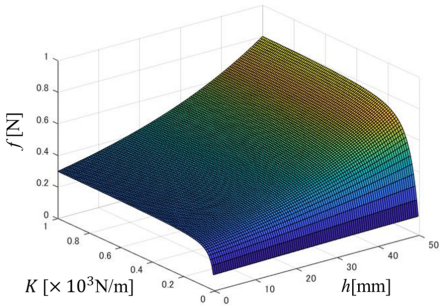

(**c**) $w_o = 15$ mm

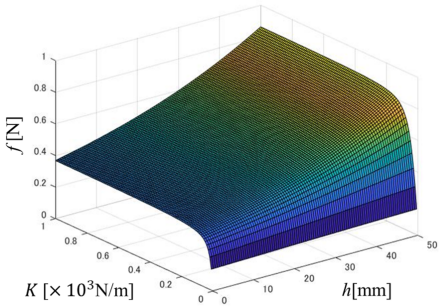

(**d**) $w_o = 20$ mm

Figure 8. Contact force related to the stiffness and the contact position as $\theta_{in} = 117.5$ deg.

5. Grasp Planning Considering the Characteristic of the Mechanism

This section addresses grasp planning utilizing the feature of the mechanism, that is the mechanism can change the contact force with changing the contact position. The proposed grasp planning derives the input motor angle and the contact position to grasp up food in order to realize a simple control system.

5.1. Grasp Planning Algorithm

The grasping of the chopstick-type gripper is modeled in order to know how much force is needed to pick up a food. The proposed mechanism is a planar mechanism, and the gripping of the target food is established by the equilibrium of forces between the gravitational force of the food and the friction forces from the gripper, as shown in Figure 9. Subsequently, the equilibrium of the forces is described as Equations (9) and (10) under the assumption that the two friction forces $F_{friction}$ are equal. In this case, m, g, μ are set as the mass of the food, the gravitational acceleration, and the coefficient of static friction, respectively.

$$2F_{friction} = mg \tag{9}$$

$$F_{friction} \leq \mu f_{gripping} \tag{10}$$

Thus, to pick up the food, the gripping force is described as Equation (11) with the safety factor $s(> 1)$ for the maximum friction force.

$$f_{gripping} = s\frac{mg}{2\mu} \tag{11}$$

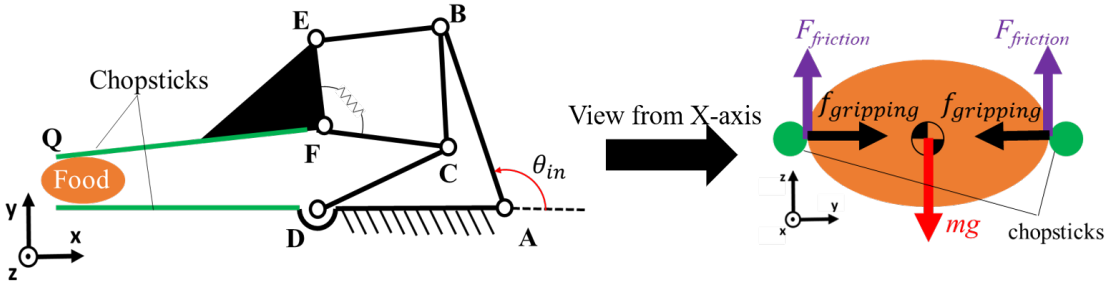

Figure 9. Simple modeling of the grasping.

In the following, the gripping force to pick up food will be obtained by the position control of the driving motor of the gripper mechanism and the end-effector of the manipulator in order to implement a simple control system, and the grasp planning is proposed based on it. In other words, the grasp planning aims to obtain the required force in order to pick up the food without feedback control.

The grasp planning algorithm is proposed from the results obtained from the analysis. In the paper, the grasp planning is regarded as the planning to decide the contact position and the input motor angle for the gripper to grasp the food. Figure 10 shows the algorithm of the proposed grasp planning. For the grasp planning, it is considered that the magnitude of the contact force $f(h) = f\cos\phi$ monotonically increases with respect to the contact position h when the stiffness of the food is known, as Figure 8 shows. Additionally, the range of contact point is set as $0 \leq h \leq h_{limit}$. The procedure of grasp planning is summarized, as follows.

1. For the given w_o, K, m and μ, the gripping force to pick up food, $f_{gripping}$, is calculated by Equation (11).
2. The motor input angle θ_{in} is given, and the function $f(h)$ is derived using the analysis.
3. It is determined if the solution h exists, which satisfies $f(h) = f_{gripping}$ in the assumed contact range ($0 \leq h \leq h_{limit}$). When the solution h exists in the range, the h is obtained by solving the equation $f(h) = f_{gripping}$. When the solution h does not exist, the motor input angle is updated and the calculation goes back to step.2.

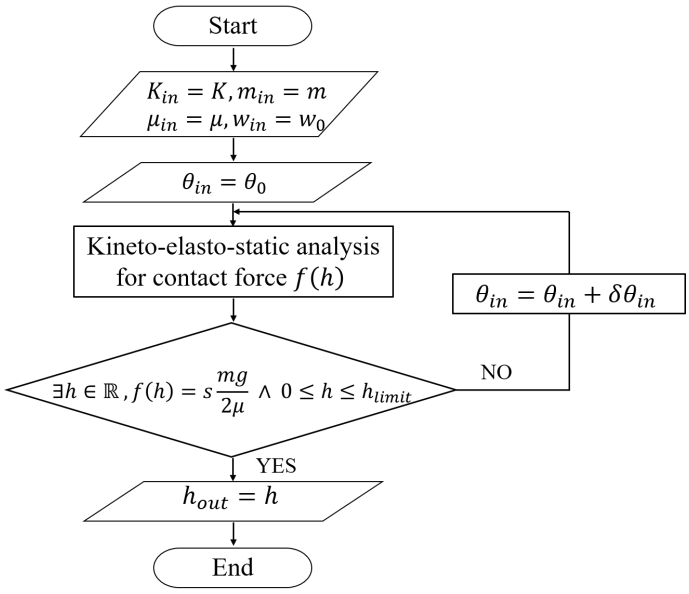

Figure 10. Flowchart of the grasp planning based on the analysis.

5.2. Case Study of the Grasp Planning

Case studies to decide the input motor angle and the contact position by the proposed grasp planning are described. For the examples, the safety factor is set as $s = 2.0$, the update value of the input motor angle is set as $\delta\theta_{in} = 1$ deg, and the range of the contact is set as $0 \leq h \leq 50$ mm.

(case.1) As $K = 0.5 \times 10^3$ N/m, $w_o = 20$ mm, $m = 0.025$ kg, $\mu = 0.40$

From Equation (11), the required force for grasping is $f_{gripping} = 0.613$ N. From Figure 11a, when the input motor angle is $\theta_{in} = 117.5$ deg, h which satisfies $f(h) = f_{gripping}$ exists, and the solution is $h = 33.43$ mm. Figure 11b shows that the calculation is converged.

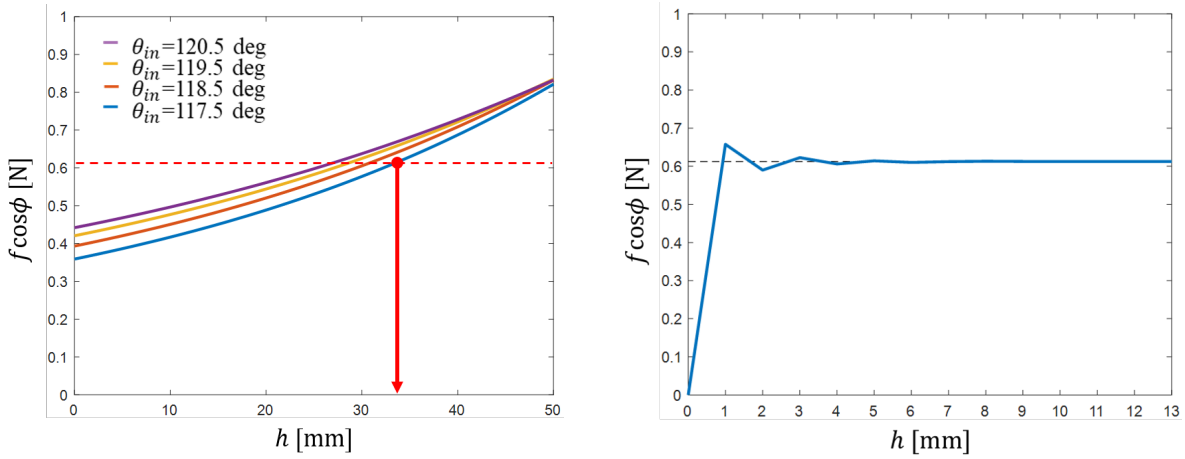

(**a**) The result of grasp point

(**b**) Convergence of the calculation

Figure 11. The result of grasp planning of case.1.

(case.2) As $K = 0.1 \times 10^3$ N/m, $w_o = 10$ mm, $m = 0.020$ kg, $\mu = 0.35$

From Equation (11), the required force for grasping is $f_{gripping} = 0.420$ N. From Figure 12a, when the input motor angle is $\theta_{in} = 117.5$ deg, h, which satisfies $f(h) = f_{gripping}$ does not exist, then the input motor angle is updated. From Figure 12a, when the input motor angle is $\theta_{in} = 118.5$ deg, the h which satisfies $f(h) = f_{gripping}$ exists, and the solution is $h = 40.89$ mm. Figure 12b shows that the calculation is converged.

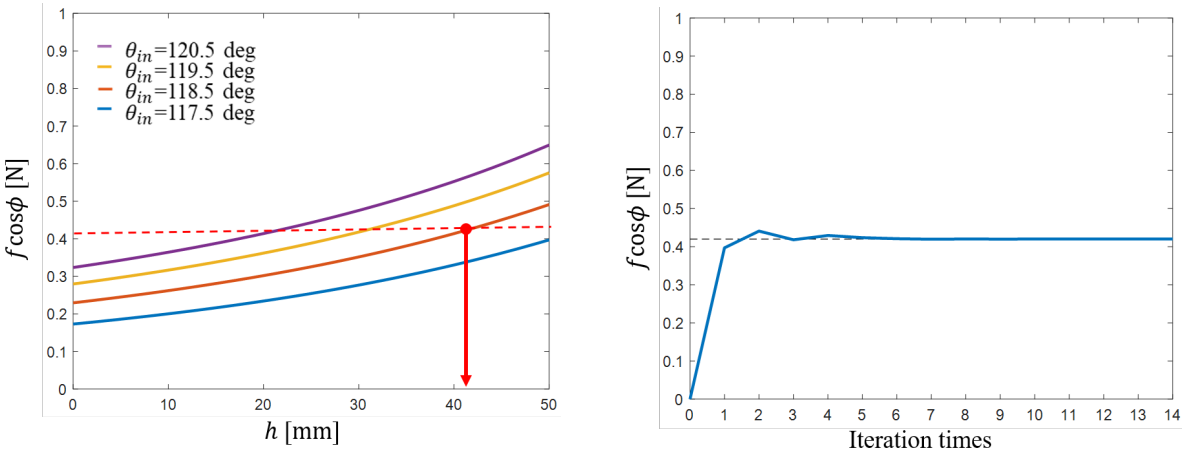

(**a**) The result of grasp point

(**b**) Convergence of the calculation

Figure 12. The result of grasp planning of case.2.

In this paper, it is assumed that the parameters of the food such as dimensions, mass and stiffness are obtained from the database based on the measurement by the vision system. Then, the error of these parameter values is inevitable. Here, let us investigate the effect of the error of stiffness value, which seems the most difficult to get precise value among the parameters, on the gripping performance through examples. The error of the stiffness K is considered under an assumption that its value includes

maximum error by 20 % of its nominal value. Two cases of nominal stiffness values: $K = 0.5 \times 10^3$ N/m and $K = 0.1 \times 10^3$ N/m for $\theta_{in} = 117.5$ deg, and $h = 5$ mm are considered. Taking into consideration the maximum 20 % error in stiffness, we obtained that the contact forces vary between 0.314 N (−0.94%) and 0.319 N (+0.63 %) (nominal value: 0.317 N) for $K = 0.5 \times 10^3$ N/m, and between 0.267 N (−3.96 %) and 0.285 N (+2.52 %) (nominal value: 0.278 N) for $K = 0.1 \times 10^3$ N/m, respectively. From these results, it is known that the sensitivity of the stiffness error on the contact force error is low while the stiffness for soft food is more sensitive to the contact force than for hard food. Therefore, it can be said that the proposed mechanism can achieve a stable gripping under the existence of the estimated stiffness value error. In the case where a quite sensitive force control is required to handle a very delicate food, in order to avoid hurting the food, a feedback control system, such as an impedance control system, may be applied. Even in such a case, a low-cost control system may be constructed by adding an angular displacement sensor at joint F to measure the spring force, which is based on the advantage of the proposed mechanism.

6. Design, Prototyping and Experiment

6.1. Design of the Prototype

The design process for determining the parameter values as shown in such as Table 1 is described. As for the design of the mechanism, the property of the food is set as Table 2. First of all, the whole size of the mechanism is determined. The length of chopstick is set on 100 mm considering on the length of real chopsticks, and the mechanism should be small enough to set as the end-effector of the meal assistance robot. In this case, the total size of two loops was set to be about 40 mm × 40 mm. Subsequently, the length of each link of Loop 1($l_{AB}, l_{BC}, l_{CD}, l_{DA}$) was determined so that the path of the chopstick part is close to the actual movement of chopsticks. Next, the length of each link of Loop 2 (l_{BE}, l_{EF}, l_{FC}) is determined, so that the larger the size of the food is, the lager the contact force outputs. At this time, the parameters were set, so that the contact force monotonously increases according to the increase of the motor input angle θ_{in} when the stiffness of food K is constant and the size is changed. In addition, the range of the motor input angle θ_{in} is set so that the tip of the chopstick part matches when the maximum θ_{in} is given in the initial loop with the grasp planning algorithm in Figure 10 when there is no target object. Finally, the spring constant of the torsion spring installed k_t was determined. The used torsion spring is a linear spring, and the order of the contact force is determined by the value of the spring constant. From Equation (11) and Table 2, the order of the required gripping force was determined and, with the safety factor $s = 2.0$, the maximum force was determined as $f_{gripping} = 0.98$ N, then the spring constant was determined. The prototype was fabricated using 3D printer as shown in Figure 13. The prototype has a double supported structure, and the actuator used for the prototype was VS-12M servo (Vigor Precision Ltd.).

Table 2. Parameter of target food.

Mass m [g]	$0 < m \leq 30$
Initial width w_o [mm]	$5 \leq w_o \leq 20$
Friction coefficient μ [-]	$0.3 \leq \mu$
Stiffness $K[\times 10^3$ N/m]	$0.01 \leq K \leq 1.0$

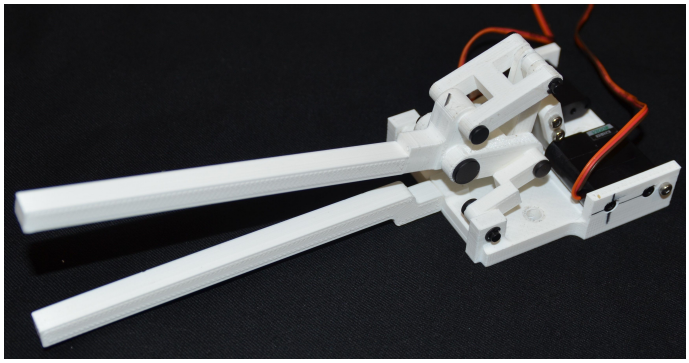

Figure 13. Gripper prototype fabricated using 3D printer (bird's eye view).

6.2. Experiment Using the Gripper Prototype with Changing the Contact Point

An experiment to measure the contact force with changing the contact position and the stiffness of the contacted object was carried out in order to validate the modeling of the mechanism including the contact point and the results of the kineto-elasto-static analysis that the gripper can change its contact force according to the size and the stiffness of food, and the contact position. In the experiment, the reaction force from the food ($K\Delta w$ [N]) was measured through a force gauge with an attachment including a compression spring, and the measured values were compared with the theoretical result of the analysis ($f \cos\phi$ [N]) based on Equation (3). Figure 14 shows the experimental setup with the gripper prototype to measure the contact force from link EFQ. The experimental setup was composed of the gripper prototype, a linear guide with a measure, and a force gauge with an attachment having a compression spring. The input angle of the motor was controlled by PWM control using a microcomputer Arduino Mega. The resolution of the motor angle was 0.1 deg. The linear guide enabled the gripper to change the contact point. The displacement was measured by the scale alongside the linear guide. The attachment of the force gauge is shown in Figure 15, and it was fabricated with a three-dimensional (3D) printer. This attachment reproduced the characteristic of the food having an stiffness and the modeling of the mechanism, as shown in Figure 3. The force gauge was DS2-20N (IMADA), and the resolution was 0.01 N. The compression spring in the attachment was replaced to change the spring constant, and the linear bushes inside the attachment made the contact point move smoothly. The experiment was carried out with changing the spring constant, using five kinds of spring, of which spring constant: 0.05×10^3 N/m, 0.1×10^3 N/m, 0.3×10^3 N/m, 0.5×10^3 N/m,and 1.0×10^3 N/m. Additionally, the contact point was changed in the area as 0 mm $\leq h \leq$ 50 mm, and the contact force was measured at every 10 mm of h. As for the input angle of the driving motor of the gripper, the input was set as $\theta_{in} = 117.5,\ 118.5,\ 119.5,$ and 120.5 deg. In the experiment, the measured values were set as the average of the five times measurement values.

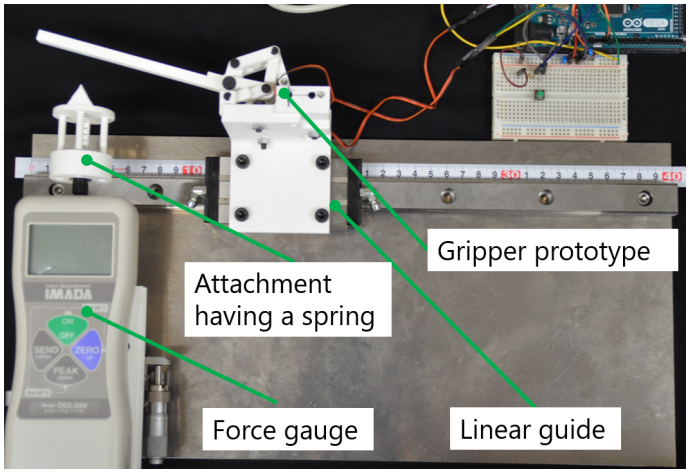

Figure 14. Experimental setup to measure the contact force with changing the contact position.

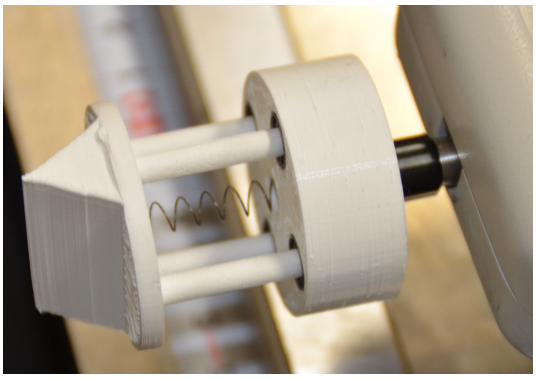

Figure 15. Attachment of the force gauge.

Figure 16 shows examples of the experimental results to measure the contact force with comparing the results of the theoretical analysis. In the figures, the theoretical value was calculated by $f\cos\phi$ [N], and the measured value was obtained by $K\Delta w$ [N] in Equation (3).The maximum difference between the measured value and the theoretical value was 0.06 N when $w_o = 15$ mm, $K = 1.0 \times 10^3$ N/m, $\theta_{in} = 120, h = 40$ mm. The main reason of these differences is considered to come from the x-component of the contact force $f\sin\phi$. In the analysis, the x-component of the contact force $f\sin\phi$ was neglected. The value is small when the value ϕ is small, so the influence seems small. However, when the ϕ becomes big, the influence of x-component of the contact force $f\sin\phi$ cannot be neglected, and the force seems to affect the movement of the attachment of the force gauge. When considering that the resolution of the force gauge was 0.01 N, the deviations between the theoretical values and measured values were small when the spring constant was set as $K = 0.05 \times 10^3$ N/m, $K = 0.1 \times 10^3$ N/m and $K = 0.5 \times 10^3$ N/m. Thus, it can be said that the analysis is validated through the experiment.

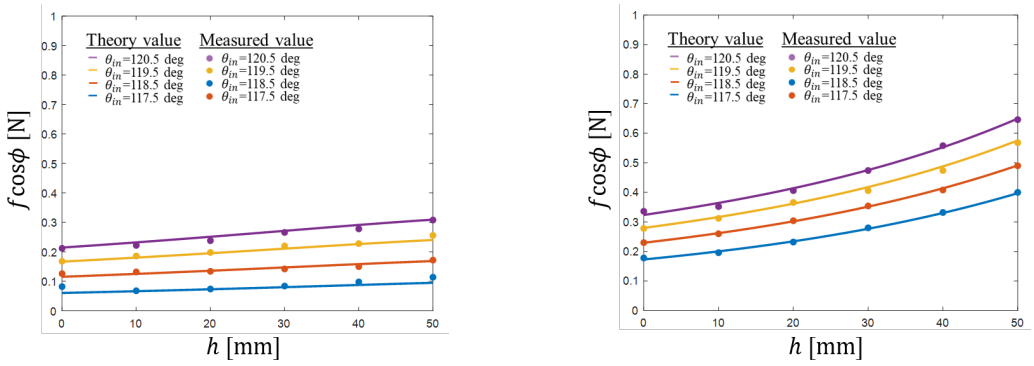

(**a**) $w_o = 5$ mm, $K = 0.05 \times 10^3$ N/m

(**b**) $w_o = 10$ mm, $K = 0.1 \times 10^3$ N/m

(**c**) $w_o = 15$ mm, $K = 0.3 \times 10^3$ N/m

(**d**) $w_o = 20$ mm, $K = 0.5 \times 10^3$ N/m

Figure 16. Comparisons between the experimental value and the theory value (Example).

6.3. Experiment of the Grasp Planning with 6-DOF Robot Arm

An experiment using 6-DOF robot arm was carried out in order to demonstrate the feasibility of the grasp planning proposed in the previous section. Figure 17 shows the experimental set up, which is composed of 6-DOF robot arm (LR Mate 200iD/4S, FANUC) and the gripper prototype, which is the same as the one used for the experiment in the previous section. The gripper prototype was implemented to the robot arm with the connected part which was fabricated by a 3D printer. In this experiment, the displacement of the gripper was controlled by the manual controller of the robot arm, and the orientation of the gripper was kept constant (the value of the orientation of the end-effector was set as $roll = 33, pitch = -67, yaw = -176$). The motor angle of the gripper was controlled through Arduino Mega, which the same one used in the previous experiment.

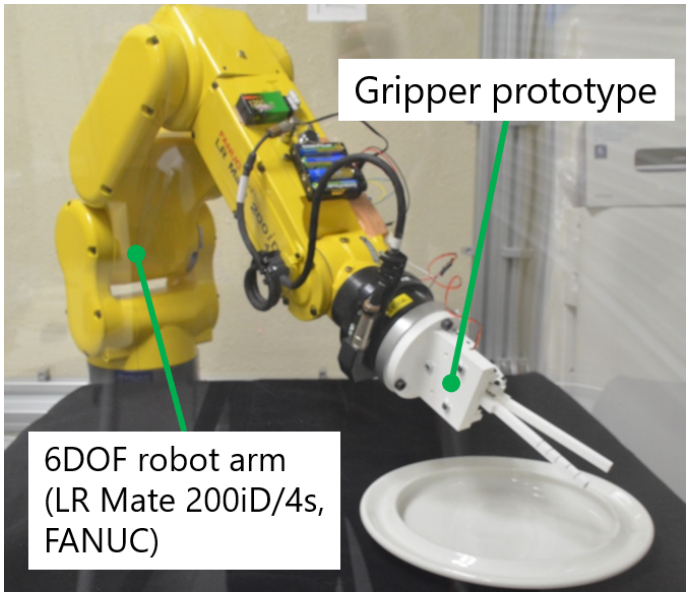

Figure 17. Experimental setup with 6-DOF robot arm

In the experiment, the target food was sushi roll, as shown in Figure 18, and the width to be grasped was measured as 16.6 mm, and the mass was measured as $m = 0.0131$ kg. From [23], the stiffness of sushi roll was obtained as $K = 0.31 \times 10^3$ N/m, and the viscosity of the food was neglected in the experiment. Additionally, the coefficient of friction was roughly set as $\mu = 0.4$ referencing [24]. From Equation (11), the required force for grasping was $f_{gripping} = 0.320$ N. From Figure 19a, when the input motor angle is $\theta_{in} = 117.5$ deg, h, which satisfies $f(h) = f_{gripping}$ exists, and the solution was obtained as $h = 2.10$ mm. Figure 19b shows that the calculation is converged.

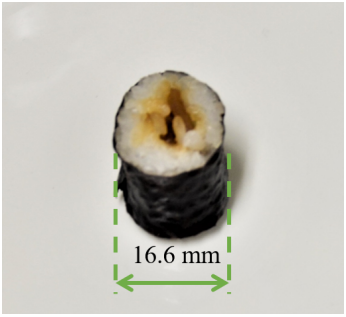

Figure 18. Target food.

Figure 20 shows the grasping experiment using the 6-DOF robot arm. From the grasp planning, the input parameters were obtained as $\theta_{in} = 117.5$ deg and $h = 2.1$ mm, and these parameters were used in the experiment. Note that the actual contact point was not point contact, and the grasping was carried out at the area where $0 \leq h \leq 10$ mm. From the figure, it was observed that the gripper successfully picked up the target food. From the result, the proposed grasp planning was confirmed to be effective under the experimental condition.

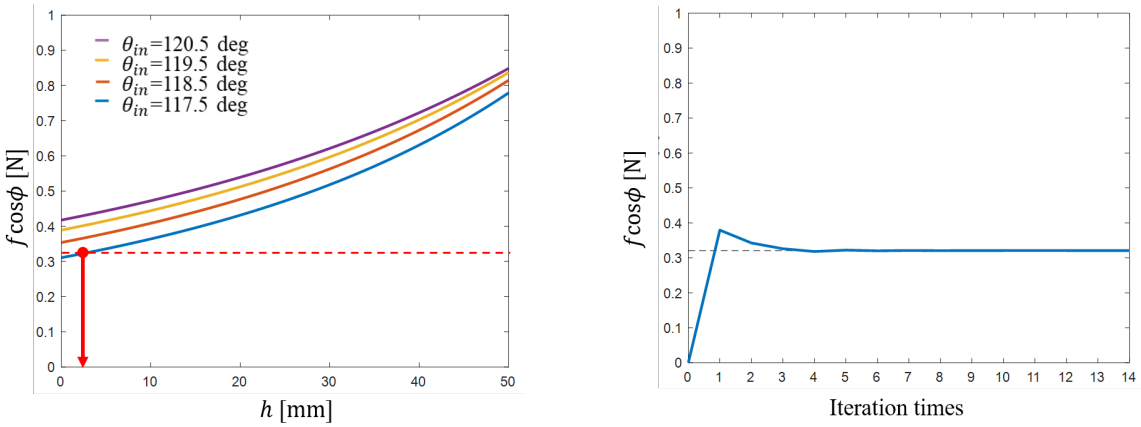

(**a**) The result of grasp point. (**b**) Convergence of the calculation.

Figure 19. The result of grasp planning.

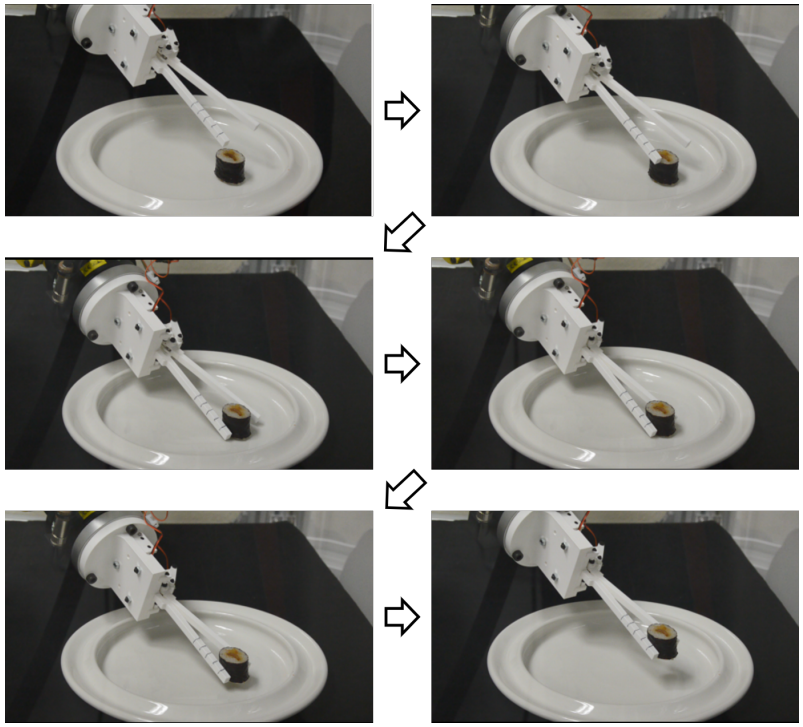

Figure 20. Grasping test with 6-DOF robot arm.

7. Conclusions

In this paper, a chopstick-type gripper mechanism based on the concept of under-actuation and solely use of position control, which is capable of adapting its shape and contact force according to size and stiffness of target foods, was proposed. Modeling of the mechanism, including the contact with target food having stiffness, has been done in order to design a practical gripper. Based on this model, an analysis scheme based on iterative calculations of kineto-elasto-static analysis has been formulated and shown to be improved through comparison with the other analysis scheme of our previous work from the point of view of the computational efficiency. Based on the result of analysis, it is revealed that the proposed mechanism is able to adjust its contact force according to the size and stiffness of target foods,

and that the gripper mechanism is able to change its gripping force according to the contact position with the target object, which is utilized for the grasp planning that determines the contact position suitable for its grasping. Through examples, it has been revealed that the contact force of the proposed mechanism is less sensitive against the stiffness error. While using the gripper prototype, the contact force was measured by a force gauge with an attachment having a spring with changing the contact point with a linear guide. From the result of the experiment, the modeling of mechanism in the kineto-elasto-static analysis and the mechanism's feature that the mechanism can change its contact force according to the size and stiffness and the contact position with the object was validated. Additionally, using the 6-DOF robot arm, the grasping test of a real food was conducted utilizing the proposed grasp planning. The gripper was able to lift up the food using the input parameters obtained by the grasp planning, and the feasibility of the grasp planning was confirmed. For future works, experiments to grasp other kinds of food will be carried out in order to decide the scope of the application of the gripper. Additionally, a control system utilizing some feedback signal without implementing complex and expensive instruments based on the impedance control will be introduced to achieve more stable and appropriate gripping a wide variety of foods. Furthermore, in addition to the gripper mechanism and its control system, future work includes the design of the gripper with different shape of the end-effector for more practical development.

Author Contributions: Conceptualization, T.O.; Investigation, T.O.; Methodology, T.O.; Project administration, J.S., A.-L.L. and Y.T. Resources, T.O., Supervision, D.M. and Y.S.; Validation, Y.T.; Writing—original draft, T.O.; Writing-Review & Editing, J.S., A.-L.L., D.M., Y.S. and Y.T. All authors have read and agreed to the published version of the manuscript.

Funding: This work was carried out as a part of the SICORP under the responsibility of the Japan Science and Technology Agency (JST) and was supported in part by JSPS KAKENHI JP17H03162.

Conflicts of Interest: The authors declare no conflict of interest.

References

1. The WHOQOL Group. The World Health Organization quality of life assessment (WHOQOL): Development and general psychometric properties. *Soc. Sci. Med.* **1998**, *46*, 1569–1585. [CrossRef]
2. Nyberg, M.; Olsson, V.; Pajalic, Z.; Örtman, G.; Andersson, H.S.; Blücher, A.; Wendin, K.; Westergren, A. Eating difficulties, nutrition, meal preferences and experiences among elderly: A literature overview from a Scandinavian context. *J. Food Res.* **2015**, *4*, 22–37. [CrossRef]
3. Topping, M.; Smith, J. The development of Handy 1, a rehabilitation robotic system to assist the severely disabled. *Ind. Rob.* **1998**, *25*, 316–320 [CrossRef]
4. Yamasaki, A.; Fukushima, M.; Masuda, R. Trial manufacture of the meal assistance robot using chopsticks and control of grasp force for foods. *Rob. Soc. Jpn.* **2012**, *30*, 917–923. [CrossRef]
5. Soyama, R. The development of meal-assistance robot 'My Spoon'. In Proceedings of the 8th International Conference on Rehabilitation Robotics, Taejon, Korea, 23–25 April 2003; pp. 88–91.
6. Secom. My spoon. Available online: https://www.secom.co.jp/english/myspoon/ (accessed on 25 January 2020).
7. Michaelis, J. Introducing the neater eater. *Action Res.* **1988**, *6*, 2–3.
8. NeaterSolutions. Neater Eater. Available online: https://neater.co.uk/neater-eater/ (accessed on 25 January 2020).
9. Products Incorporated 2003, R. Meal buddy. Available online: http://www.richardsonproducts.com/mealbuddy.html (accessed on 25 January 2020).
10. Copilusi, C.; Ceccarelli, M. An application of LARM clutched arm for assisting disabled people. *Int. J. Mech. Control* **2015**, *16*, 57–66.
11. Song, W.K.; Kim, J. Novel assistive robot for self-feeding. *Rob. Syst. Appl. Control Program.* **2012**, *1*, 43–60.
12. EU-Japan Centre for Industrial Cooperation. Japan-Sweden Academia-Industry International Collaboration. Available online: https://www.eu-japan.eu/news/bilateral-call-japan-sweden-academia-industry-international-collaboration (accessed on 25 January 2020).

13. Norén A-L. Bestic: An Eating-Aid for Persons with Little or No Ability to Move Their Arms. Master's Thesis, Chalmers University of Technology, Gothenburg, Sweden, 2005.
14. Lindborg, A.L.; Lindén, M. Development of an eating aid - from the user needs to a product. *Stud. Health Technol. Inf.* **2015**, *211*, 191–198.
15. Solis, J.; Karlsson, C.; Ogenvall, M.; Lindborg, A.L.; Takeda, Y.; Zhang, C. Development of a vision-based feature extraction for food intake estimation for a robotic assistive eating device. In Proceedings of the 2018 IEEE 14th International Conference on Automation Science and Engineering (CASE). Munich, Germany, 20–24 August 2018; pp. 1105–1109.
16. Birglen, L.; Gosselin, C.M. Kinetostatic analysis of underactuated fingers. *IEEE Trans. Rob. Autom.* **2004**, *20*, 211–221. [CrossRef]
17. Stavenuiter, R.A.; Birglen, L.; Herder, J.L. A planar underactuated grasper with adjustable compliance. *Mech. Mach. Theory* **2017**, *112*, 295–306. [CrossRef]
18. Fukaya, N.; Asfour, T.; Dillmann, R.; Toyama, S. Development of a five-finger dexterous hand without feedback control: The TUAT/Karlsruhe humanoid hand. In Proceedings of the 2013 IEEE/RSJ International Conference on Intelligent Robots and Systems, Tokyo, Japan, 3–7 November 2013; pp. 4533–4540.
19. Ueno, T.; Oda, M. Development of an index finger for the dexterous hand for space. *J. Rob. Soc. Jpn.* **2010**, *28*, 349–359. [CrossRef]
20. Oka, T.; Matsuura, D.; Sugahara, Y.; Solis, J.; Lindborg, A.; Takeda, Y. Chopstick-type Gripper Mechanism for Meal-Assistance Robot Capable of Adapting to Size and Elasticity of Foods. In *Mechanism Design for Robotics*; Springer: Cham,Switzerland, 2018; pp. 284–292.
21. Suwa, T.; Iwatsuki, N.; Ikeda, I. Kinematic Analysis and synthesiS of Flexible Mechanism Composed of Underactuated Mechanism Constrained with Elastic Element. In Proceedings of the Mechanical Engineering Congress, Hokkaido, Japan, 14 September 2015; S1170203.
22. Iwatsuki, N.; Kotte, T.; Morikawa, K. Simultaneous control of the motion and stiffness of redundant closed-loop link mechanisms with elastic elements. *J. Mech. Sci. Technol.* **2010**, *24*, 285–288. [CrossRef]
23. Sakamoto, N.; Yuya, M.; Higashimori, M.; Kaneko, M. An Optimum Design for Handling a Visco-elastic Object Based on Maxwell Model. *J. Rob. Soc. Jpn.* **2007**, *25*, 166–172. [CrossRef]
24. Editorical Commitee of "Shokuhin-kagaku-binran". *Shokuhin-Kagaku-Binran*; Kyoritsu Shuppan Co, Ltd.: Tokyo, Japan, 1978; p. 265. (In Japanese)